

ATLAS Silicon Microstrip Semiconductor Tracker (SCT)

Y.Unno^a, representing the ATLAS SCT collaboration¹

^aKEK, Oho 1-1, Tsukuba, Ibaraki 305-0801, Japan

Abstract

Silicon microstrip semiconductor tracking system (SCT) will be in operation in the ATLAS detector in the large hadron collider (LHC) at CERN. Challenging issues in the SCT are the radiation tolerance to the fluence of 2×10^{14} 1-MeV-neutron-equivalent particles/cm² at the designed luminosity of 1×10^{34} cm⁻²/s of the proton-proton collisions and the speed of electronics to identify the crossing bunches at 25 ns. The developments and the status of the SCT are presented from the point of view of these issues. Series production of the SCT will start in the year of 2001 and the SCT will be installed into the ATLAS detector in the year of 2003-2004.

I. INTRODUCTION

The large hadron collider (LHC) is under construction at CERN, using the existing LEP tunnel of 27 km circumference, in order to accelerate protons to 7 TeV and to make head-on collisions at the center-of-mass energy of 14 TeV with a luminosity of 10^{34} cm⁻²s⁻¹ [1]. The ATLAS detector, one of the two major general purpose detectors in LHC, was approved as an experiment in 1994 and is planned to be in operation in 2005 [2]. Its tracking detector near the interaction point, the inner detector, was approved for construction in 1997 [3].

The inner detector tracks charged particles inside a solenoidal magnet, identifies particle trajectories and measures momentum in the magnetic field. The required design precision in spatial resolution, radiation tolerance, and particle separation have been addressed by the use of semiconductor devices in the inner part and gas-drift chambers with transition radiation capability (TRT) in the outer part. The semiconductor devices are further split into the Silicon pixel devices (Pixels) in the innermost region and the Silicon microstrip devices (SCT) in the central region between the Pixels and TRT.

The issues, status of development, and schedule of the SCT are described based on developments in the barrel section.

II. DETECTOR OVERVIEW

A. ATLAS

An overview of the ATLAS detector is shown in Figure 1. The full detector is 22 m high, 46 m long, and weighs 7000 t which approximately comprises the inner detector of 4 t, Liq.Ar calorimeter 700 t, Tile calorimeter 4000 t, Muon chambers

500 t, the solenoid 3 t, Air-core toroids 1300 t, and the supports 500 t. The concept of the detector is to measure precisely (with major goals in parenthesis)

1. the momentum of muons outside the calorimeter using the magnetic field generated by the air-core superconducting toroidal magnets (for measuring the Higgs particle decays, $H \rightarrow \mu\mu\mu\mu$),
2. the electromagnetic particles, such as electrons, positrons, and γ 's, with a radiation tolerant calorimeter (for measuring $H \rightarrow \gamma\gamma$),
3. the missing hadronic energy with a hadronic calorimeter (for identifying SUSY particle decays, $SUSY \rightarrow$ normal particles + missing energy), and
4. the charged particles, inside the calorimeter, using a solenoidal magnetic field (for identifying b- and tau- particles, and event topologies).

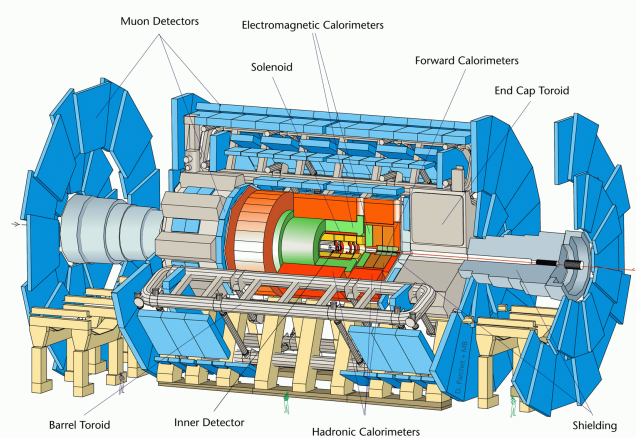


Figure 1: Overview of ATLAS detector at LHC

B. Inner detector

Although tiny compared to the full ATLAS detector, the inner detector is still large and complex: 2.3 m in diameter, 7 m in length. The detection elements are, from the interaction point, Pixel detectors (3 layers), the Semiconductor tracker (SCT) which is based on Silicon microstrip detectors (4 layers), and Transition Radiation Tracker (TRT) based on straw drift tubes

¹Univ. Melbourne, Univ. Sydney, Australia; Acad. Scie. Czech Rep., Czech Tech. Univ., Charles Univ., Czech; Univ. Freiburg, MPI Munich, Germany; NIKHEF, Holland; Hiroshima Univ., KEK, Kyoto Univ. Edu., Okayama Univ., Univ. Tsukuba, Japan; Univ. Bergen, Univ. Oslo, Norway; INP Cracow, FPNT Cracow, Poland; Moscow State Univ., IHEP Protovino, Russia; Univ. Ljubljana, Slovenia; Univ. Valencia, Spain; Univ. Uppsala, Sweden; Univ. Bern, CERN, Univ. Geneva, Switzerland; Univ. Birmingham, Univ. Cambridge, Univ. Glasgow, Lancaster Univ., Univ. Liverpool, Univ. Manchester, Oxford Univ., QMW, RAL, Sheffield Univ., UCL, UK; Univ. California-Irvine, LBNL, Univ. California-Santa Cruz, Univ. Wisconsin, US

with interleaved transition radiator made of polypropylene foils (64 layers or more). The layout is shown in Figure 2.

The function of the inner detector is to track the charged particles in the 2 Tesla solenoidal magnetic field. The major issues in the tracking are:

1. Precision measurement of positions in order to identify the trajectories, measure the momenta, and identify the charge of particles, where the required precision enables charge identification up to 500 GeV/c,
2. Enhancing electron identification capability for heavy particle identification,
3. Speed of electronics in order to tag the bunches which cross every 25 ns,
4. Radiation tolerance to the fluence of charged and neutral particles liberated from the primary interactions and from the walls and the calorimeters, in order to survive for 10 years of operation,
5. Amount of material which scatters the particles and introduces inaccuracy in the measured momentum and energy, and
6. Cost.

The layout of the inner detector is the result of optimization by the ATLAS collaboration. The position resolutions in the $r\phi$ direction are $12 \mu\text{m}$ / layer in the Pixels, $16 \mu\text{m}$ / layer in the SCT, and $28 \mu\text{m}$ / 36 straws per track in the TRT.

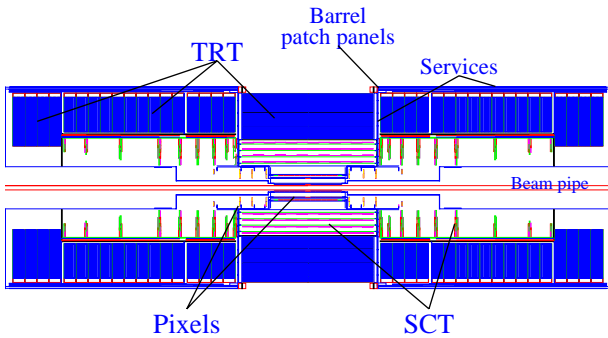


Figure 2: Layout of the inner detector

C. SCT (Silicon microstrip semiconductor tracker)

The SCT, covering the pseudo-rapidity range -2.5 to $+2.5$ with four layers of cylinders in the barrel and 9 layers of disks in each of the forward sections, requires an area of 61 m^2 of Silicon microstrip sensors. The precision of the SCT is achieved with a strip pitch of $80 \mu\text{m}$, a pair of sensor layers being arranged within a module to have a small stereo angle of 40 mrad resulting in a resolution of,

$$\sigma(r\phi) \sim (80\mu\text{m}) / (\sqrt{12}) / (\sqrt{2}) = 16\mu\text{m}.$$

Minimization of cost and electronics channels in balance with the occupancy of hits in a strip resulted in using two near-square sensors daisy-chained to form a strip length of 12 cm. The microstrip sensors have a size of 63.6 mm (width) x 64.0 mm (length) with strip length of 62.0 mm , which is a maximum size to be made out of a 4-inch Silicon wafer. The layout of the sensor is shown in Figure 3. A number of fiducial marks are implemented in the surrounding edges for alignment and identification. The sensors have 768 readout strips, each with integrated AC-coupled metalised strips.

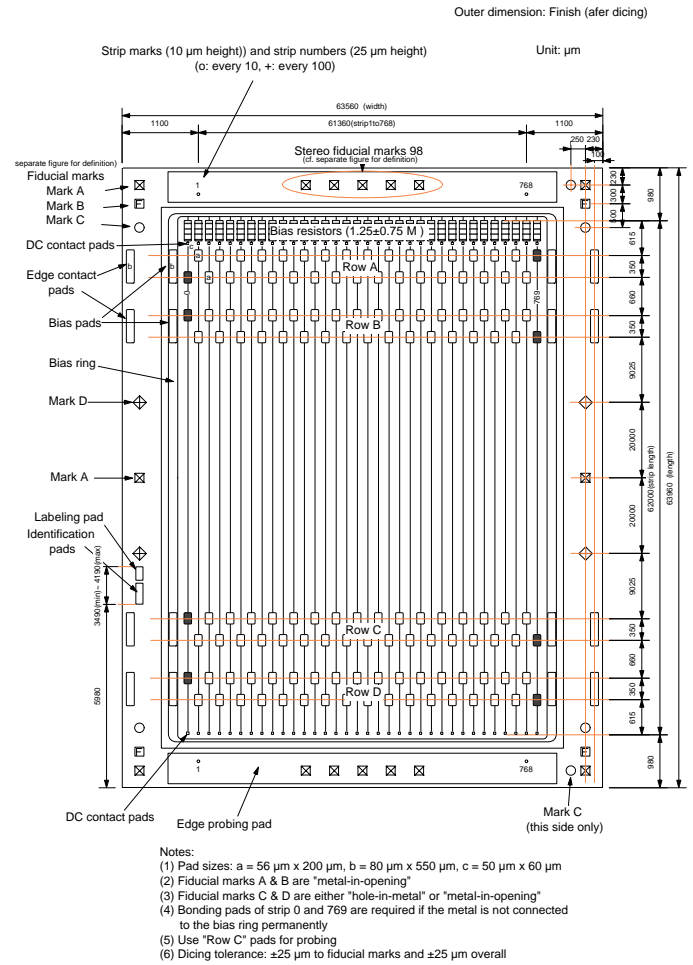


Figure 3: Layout of the Silicon microstrip sensor in the barrel section of the SCT

D. Radiation tolerance

At the design luminosity of $1 \times 10^{34} \text{ cm}^{-2} \text{ s}^{-1}$ proton-proton collisions, the annual fluence of charged and neutral particles has been estimated. The total fluence, expressed as the fluence of neutrons of 1 MeV kinetic energy giving equivalent non-ionizing damage, is shown in Figure 4. There is a systematic uncertainty of 50% due to the uncertainties in the proton-proton cross sections, etc. The cumulative fluence over 10 years can be calculated by assuming LHC operation at a low luminosity of

$1 \times 10^{33} \text{ cm}^{-2} \text{ s}^{-1}$ in the first 3 years and a high luminosity of $1 \times 10^{34} \text{ cm}^{-2} \text{ s}^{-1}$ in the remaining 7 years.

At the inner-most radius of the barrel section of the SCT, $r=30 \text{ cm}$, the annual fluence is $\sim 1.8 \times 10^{13} \text{ n/cm}^2 / \text{yr} / L=10^{34}$. In 10 years, including the 50% uncertainty in the fluence, the 1-MeV neutron equivalent fluence is $\sim 2 \times 10^{14} \text{ n/cm}^2$. For charged particle damage, since the damage by protons of more than several GeV/c is about 60 to 70% of the damage by 1-MeV neutrons, the fluence of protons of $\sim 3 \times 10^{14} \text{ p/cm}^2$ must also be considered when testing the radiation tolerance.

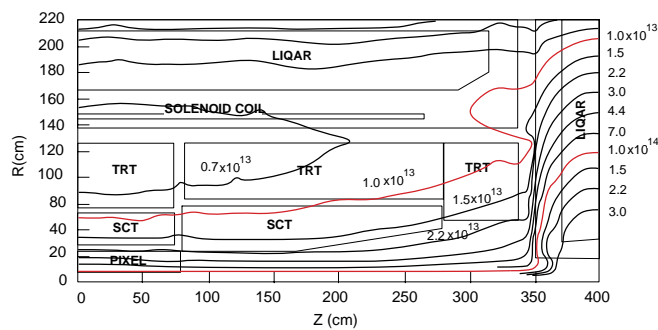


Figure 4: Yearly fluence of charged and neutral particles, translated into the 1-MeV neutrons, in the inner detector

III. DEVELOPMENT AND STATUS OF SCT

A. Radiation-hard Silicon microstrip sensor

The SCT collaboration has been involved in the development of radiation-hard Silicon microstrip sensors for a number of years. Developments in understanding the radiation damage, in sensor designs, and understanding of the cost, has led the collaboration to reach a final design choice.

Historically, the collaboration first chose single-sided n-strip readout in the n-bulk Silicon, n-in-n sensors, over double-sided sensors. The basic arguments for the choice were the understanding of the full depletion voltage being over 300 V for a 300 μm thick Silicon wafer after the SCT fluence, mutation of the bulk from the n- to p-type, and a high voltage to the integrated AC coupling (or floating one side of the readout electronics) in the double-sided case. The n-in-n single-sided sensor provides operation with null voltage to the AC coupling and a capability of partially depleted operation since the p-n junction is at the strip side after type inversion. Although n-in-n sensors have a good operational margin in radiation tolerance, they require a double-sided manufacturing process.

The commonly used single-sided Silicon microstrip sensors in high-energy physics experiments are the p-strip readout in n-bulk Silicon, p-in-n sensors. These sensors have a cost advan-

tage over the n-in-n sensor since the backside manufacturing process is simpler. More recent developments in understanding of the radiation damage to the p-in-n sensor and in the structures which withstand the high bias voltage and the high electric field around the strip edges have shown that p-in-n design still work sufficiently well after the full expected fluence in the SCT. Charge collection measurements in a beamtest and with a beta-source, noise measurement, etc., have confirmed that the performance of p-in-n sensors satisfies the requirements of the SCT. The SCT collaboration has decided on the p-in-n sensor as its final choice.

An example of the leakage current characteristics of the latest design, the so-called “wide-metal p-in-n sensor” [4], is shown in Figure 5. Ten sensors were irradiated to 3×10^{14} protons/cm², annealed to the equivalent of 10 years operation [5], and measured at $-18 \text{ }^\circ\text{C}$. The figure shows six samples. The leakage currents are, although gradually increasing, smooth up to a bias voltage of 500 V. All 10 samples irradiated showed similar characteristics.

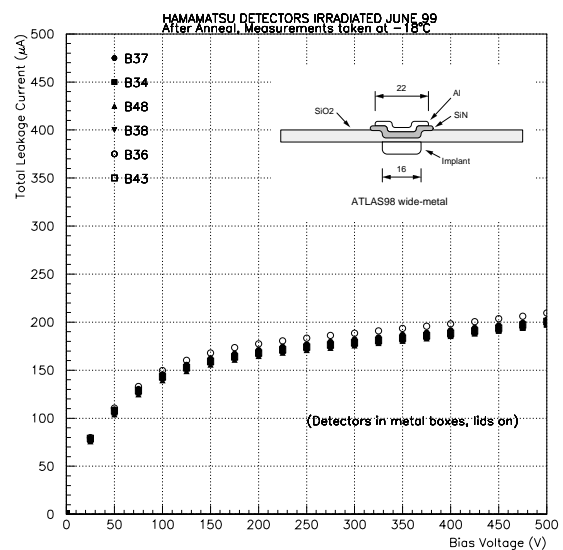


Figure 5: Leakage current vs bias voltage of the wide-metal design of the p-in-n sensor of the SCT, after $3 \times 10^{14} \text{ protons/cm}^2$ damage

The inset of Figure 5 shows the strip structure of the wide-metal sensor. The passivation layer made of SiO_2 over the top surface is not shown. The electric field concentrates at the strip edge. If the electric field strength exceeds the avalanche breakdown voltage of the material, it will generate increased leakage current and electric noise: the onset of microdischarge [6]. A tiny defect at the edge also makes the field concentrate and initiates breakdown even earlier. In the SCT, the implant and the metal strips are operated at the same potential. In this case, when the metal is wider than the implant strip, the concentration of the electric field is at the edge of the wider electrode which is inside the SiO_2 whose avalanche breakdown voltage is an order greater than that of Silicon.

Other characteristics confirmed in the irradiated samples were long-term stability of leakage current over 24 hours, with no surprises, and the small number of shorts in the AC coupling, which was also excellent. The number of shorts in the samples is summarized in Table 1. A single sensor has 768 strips and the average fraction of shorts was slightly above 0.2% even after applying 100 V voltage to the AC coupling capacitors.

Table 1.
Number of shorts in AC coupling. The voltage in the “After ()” is the voltage applied to the AC coupling capacitors.

	Irradiation	Before	After (10V)	After (100V)
Sample 1	April 99	0	0	0
Sample 2	April 99	0	0	2
Sample 3	April 99	0	0	1
Sample 4	June 99	0	1	1
Sample 5	June 99	0	3	3
Sample 6	June 99	1	1	3
Average fraction		0.02%	0.11%	0.22%

B. Silicon microstrip sensor production

One type of Silicon microstrip sensor geometry is sufficient to cover the cylindrical geometry in the barrel region of the SCT efficiently, while 5 different wedge-shaped sensor geometries are required for the disk geometry in the forward region. SCT has chosen a thinner sensor, 260 μm , in the inner-most part of the barrel and forward, and a thicker (but slightly thinner than standard) 285 μm sensor for the remaining layers, in order to reduce the depletion voltage. The sensor mnemonics, thickness, and quantity are listed in Table 2. Production of 19,440 sensors are shared by Hamamatsu photonics, SINTEF, CiS, and CSEM. Pre-series production of 5% is to be evaluated by Aug. 2000 and full production is to be completed by the 3rd Quarter of 2002.

C. Readout electronics

Another challenging area in the SCT is the readout electronics adjacent to the sensors, within the fiducial volume. The architecture chosen is one of threshold discrimination, known as “binary” readout, for simplicity and cost. The major goals of the electronics are:

1. Signal-to-noise ratio > 12 , with the noise $< 1500 e$,
2. Speed for tagging the 25 ns bunch, which sets the time walk < 16 ns,
3. Double pulse separation, < 50 ns, for minimizing the dead time,
4. Threshold uniformity $< 4\%$ (1 sigma) for assuring low noise occupancy,
5. Electrical stability of the fully-populated module, and

Table 2
Number of Silicon microstrip sensors in the SCT including 20% spares

Barrel		10,560
B1	260 μm	1,920
B2	285 μm	8,640
Forward		8,880
W12	260 μm	1,000
W21	285 μm	1,400
W22	285 μm	1,600
W31	285 μm	2,340
W32	285 μm	2,340

6. Radiation tolerance.

A schematic of the functionality of the front-end electronics is shown in Figure 6. Each channel is a chain of two blocks: the first block contains amplification, integration, uni-polar shaping, and discrimination, and the second block buffering the binary signals in a memory of 132 depth during the readout trigger latency (level 1 trigger), and a readout buffer. A chip consists of 128 channels and control sections. The control sections receive the clock, commands, and readout triggers, and also contain digital-to-analogue converters to set the voltages and currents for the threshold and front-end transistors. The chip is clocked at the same frequency as the LHC, 40 MHz.

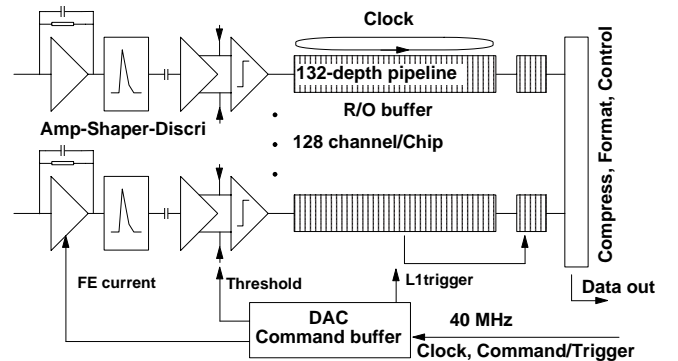


Figure 6: Schematic of the functionality of the front-end electronics

The high-speed amplification sections are best suited to Bi-polar technology while the memories and the control sections are suited to CMOS technology. Development of radiation-tolerant front-end electronics has been pursued along two paths: full functionality in one BiCMOS process, the one-chip solu-

tion, and separated functionality in Bipolar and CMOS processes, the two-chip solution. The ASICs in the one-chip solution are known as ABCD [7] and the two-chip as CAFE and ABC [8].

In the ABCD design, after experience obtained with the first generation of chips, the threshold uniformity was improved by introducing a 4 bit DAC to each channel for fine adjustment of the threshold voltage. This second generation chip is known as ABCD2T (for “trimmed”). An example of the threshold uniformity from the barrel module described in section D is shown in Figure 7. The sigma of the uniformity is 3.2 mV, which is about 6% at an equivalent threshold of 1 fC, with a gain of about 55 mV/fC. There are a number of channels outside this uniformity band which is one of the remaining issues to be resolved.

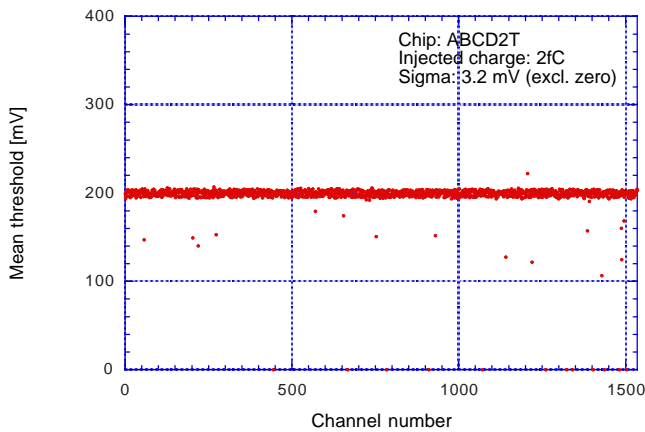


Figure 7: Uniformity of threshold in a module with 1536 channels

Radiation tolerance has been extensively evaluated: ionization damage with gamma rays to a dose of 10 Mrad, and non-ionization damage with 1 MeV-equivalent neutrons to a fluence of 2×10^{14} n/cm²: done with 24 GeV protons to 3×10^{14} p/cm² at an accelerator and 10 MeV neutrons from a reactor to 2×10^{14} n/cm². The major types of radiation damage in the chips are: degradation of beta in Bipolar-Junction-Transistors, V_t shift in MOSFET's, and increase of resistance in resistors. Results are that ABCD2T and CAFE chips certainly almost met requirements, but are still being evaluated as to whether all requirements are fully met, such as noise, channel-to-channel matching, time-walk, etc. Studies with more statistics are also under way.

D. SCT Silicon strip barrel module

The basic unit of SCT Silicon microstrip sensors and associated front-end electronics is known as a module. The construction of a module for the barrel section is shown in Figure 8. Two 6.4 cm square sensors are aligned to form a 12 cm strip unit. Two such pairs are aligned and glued on the top and the bottom of the central core, the baseboard, at an angle of 40 mrad to make the stereo measurement.

The baseboard acts as a mechanical core and also to transfer the heat of the front-end electronics and the sensors to the cooling pipe which is fitted to one edge of the baseboard. A good heat transfer capability is critical in order prevent thermal runaway in the sensors. The baseboard is also used as a conductor to provide bias voltage to the backplane of the sensors. The material chosen for the baseboard is a Carbon material called TPG [9] which has a very good thermal conductivity of 1700 W/m/K in plane and a low radiation length.

The front-end ASICs are mounted on hybrids set near the centre of the module, one above and one below the sensors. The two hybrids are connected to each other by a wrap-around inter-connection and to the external world by an inter-connection at the cooling end. Although not easily visible in the figure, a unique feature of the module is that the hybrid substrate has a steps at each end and is bridged over the sensors with a thin air gap; the hybrid is not glued to the surface of sensors but to the protruding edges of the baseboard. Electrical connections between the sensors and between the sensors and the hybrids are by Aluminium-wire bonding. The concept of the forward modules is similar except that the hybrids are mounted at the end of the module and cooling contacts are in the middle of the hybrids to suit the constraints of the disk geometry.

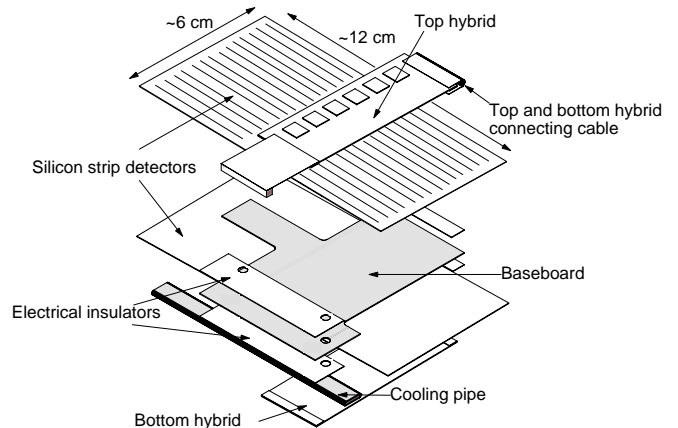


Figure 8: Construction of the barrel module

A full module has been fabricated, using ATLAS-specification Silicon microstrip sensors, ABCD2T chips and a Kapton hybrid. The Kapton hybrid is a four layer lamination of Copper and Polyimide films, which allows one-piece construction of hybrids and inter-connections, thus eliminating vulnerable extra glued or soldered connections and assuring good electrical continuity from the backside hybrid to the connection at the cooling end. The fabricated module is shown in Figure 9, housed in an Aluminium frame and connected to a communication card for testing. The module, although not irradiated, shows good performance, such as the uniformity of threshold shown in Figure 7, and stable operation down to the maximum of the pedestal noise.

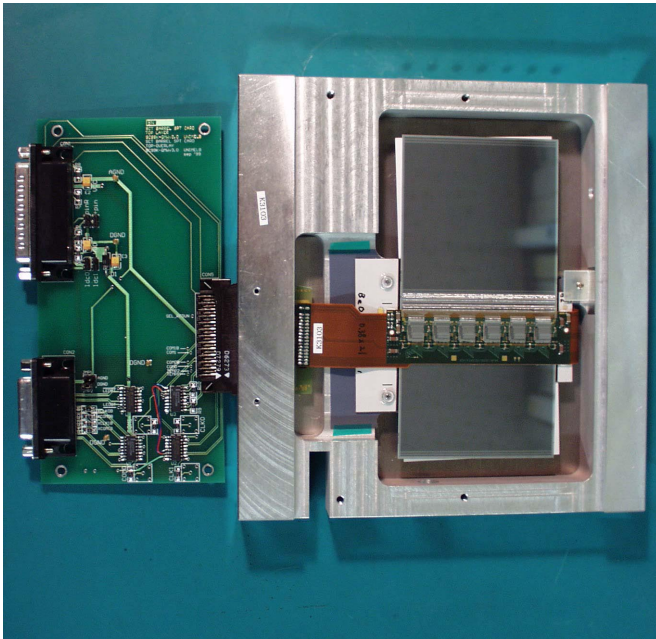


Figure 9: Fabricated barrel module being set in an Aluminium frame together with a communication card for testing

In designing the module, major issues have been three separate stabilities: electrical, mechanical, and not least thermal. During the projected lifetime of 10 years of the SCT microstrip sensors, the leakage current is expected to increase several orders of magnitude from a very low initial current, and the full depletion voltage to several hundred volts, due to the radiation damage. The Silicon microstrip sensors are to be operated around $-7\text{ }^{\circ}\text{C}$ in order to reduce the leakage current and to minimize the increase of full depletion voltage. Because of the positive feedback of the temperature and leakage current, and although the module is to be operated cold, the current and the temperature would increase very rapidly if not cooled below a critical temperature, a very serious effect known as thermal runaway.

A thermal finite element analysis (FEA) has been made to the barrel module. The hottest temperatures in the sensors are shown in Figure 10, as a function of the heat flux, normalized at $0\text{ }^{\circ}\text{C}$, parameterized for several coolant temperatures. Thermal runaway occurs when the temperature is about $10\text{ }^{\circ}\text{C}$ higher than that of null heat flux in the sensor. The heat flux required to raise the temperature by $10\text{ }^{\circ}\text{C}$ depends on the coolant temperature. The nominal heat flux normalized at $0\text{ }^{\circ}\text{C}$ is about $100\text{ }\mu\text{W}/\text{mm}^2$ at a bias voltage of 350 V . In order to expel the thermal runaway above $200\text{ }\mu\text{W}/\text{mm}^2$, the coolant temperature must be below $-15\text{ }^{\circ}\text{C}$.

The numbers of modules required in the SCT is summarized in Table 3. The SCT system is made of 4088 modules in total, 2112 modules in the barrel and 1976 modules in the forward sections. In addition, a 10% supply of spare modules are to be fabricated. Production of the modules is scheduled to start in 2001 and to be completed in 2 years, with manufacture at 4 as-

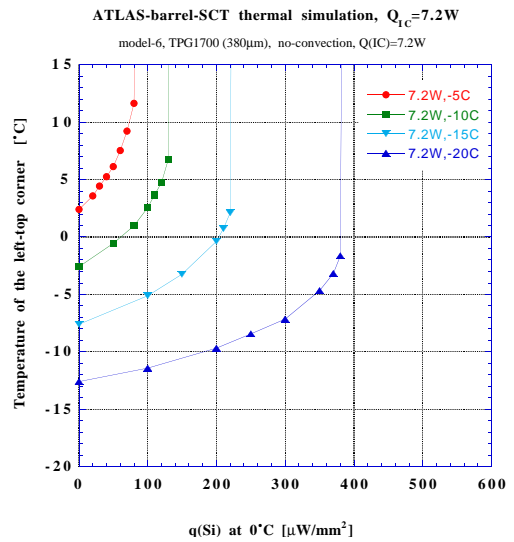


Figure 10: Thermal finite element analysis of the barrel module

sembly sites for the barrel and 3 for the forward sections. The production rate must be about 8 modules per week per site to meet the schedule.

Table 3
Number of modules in the SCT

Barrel		2112
Layer	Radius [mm]	Modules
B1	300	384
B2	373	480
B3	447	576
B4	520	672
Forward		1976
Disk	Z [mm]	Modules
2xD1	± 835	264
2xD2	± 925	184
2xD3	± 1072	264
2xD4	± 1260	264
2xD5	± 1460	264
2xD6	± 1695	264
2xD7	± 2135	184
2xD8	± 2528	184
2xD9	± 2778	104
Total		4088

E. Barrel cylinder assembly

The fabricated modules are to be positioned precisely on cylindrical support structures in the barrel and on the disks in the forward sections. A graphical view of a barrel cylinder (B1) is shown in Figure 11, an illustration obtained by encoding the geometry in the Geant4 program [10]. In order to prevent a hole in detection of particles from the interaction point, adjacent modules are overlapped about 500 μm at each end. Adjacent modules in a row are staggered with a separation of 1 mm in radius, and are tilted at 10° to allow overlap of adjacent rows.

Since the clearance between the modules is very small, and the number of modules is large, a module-mounting robot is being developed. Photographs of the robot and the robot in action are shown in Figure 12. The function of the robot is not only to carry the modules into their final positions as targeted by CCD cameras, but also to place and tighten dowel screws with which they are mounted to a pre-determined torque. The robot is made from 6 linear motions, 2 rotations, and 4 pressure-driven strokes. Two of the linear motions and one rotation are programmed to move simultaneously, a 3-axis motion, in order to carry the module into the final position safely and precisely.

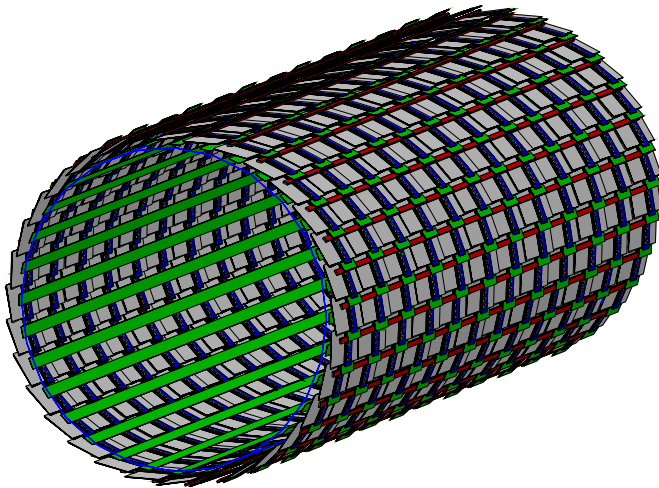


Figure 11: A graphical view of the barrel cylinder (B1). The carbon-fibre support cylinder is shown as a circle in an end.

F. Schedule

The construction schedule of the SCT, as of November 1999, is shown in Figure 13. In order to meet the turn-on deadline of the ATLAS detector in 2005, the installation of the inner detector in the experiment is scheduled for the 2nd Quarter (Q2) of 2004, and therefore the installation of the SCT into the inner detector is planned for the Q1 of the same year.

Major items of the construction of the SCT are grouped into four categories: Macro assembly, Modules, Off-detector, and System test. Macro assembly, installation of modules on the cylinders and disks, is scheduled to begin in the Q3 of 2001 and completed by the Q3 of 2003. For the fabrication of modules,

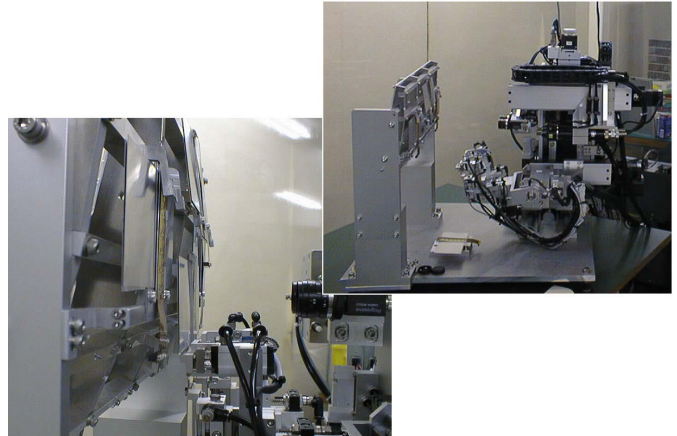


Figure 12: Module-mounting robot for the barrel cylindrical support structure. Top inset: overview together with a section of a dummy cylinder for development, and the bottom inset: the robot in action, holding a dummy module and moving toward the final position.

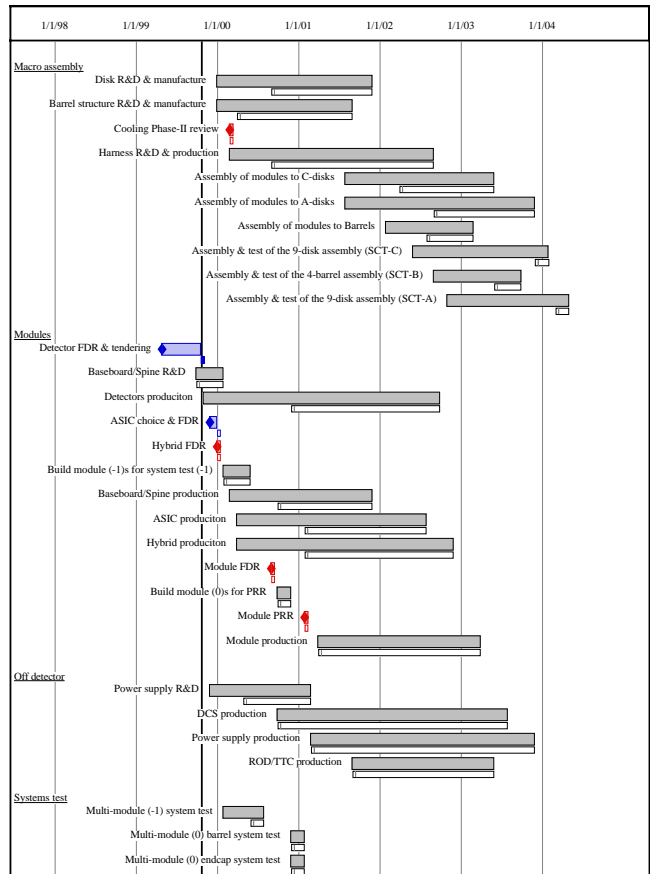


Figure 13: Construction schedule of the SCT, as of November 1999. The date in the top row is in day/month/year.

pre-production of Silicon microstrip sensors starts at the end of

1999, series production in the Q3 of 2000, and is to be completed by the Q3 of 2002. Production of the front-end electronics ASICs is to start later than the sensor production but is to be completed earlier. Module assembly follows the series production of sensors and ASICs, and is to be completed by the 1st Quarter (Q1) of 2003. Verification of the SCT with prototype setups, the system tests, are scheduled for 2000 in order to permit the start of these construction processes at the beginning of 2001.

IV. SUMMARY

The ATLAS detector, exploring the physics of Higgs and other particles in TeV energy region, is under construction. One of the precision charged particle tracking devices near the interaction point inside the solenoidal magnetic field is the SCT, based on the Silicon microstrip sensor technology. Understanding of, and developments in, Silicon microstrip sensors have shown that p-readout microstrip sensors in n-bulk Silicon can survive radiation damage to a fluence of 2×10^{14} 1-MeV equivalent neutrons/cm².

A front-end electronics system using on/off “binary” readout with buffering memories which store the “hit” information during the first level trigger latency has been demonstrated. Three types of radiation-hard ASICs are under development: one with full functionality in one chip, ABCD using a BiCMOS rad-hard process; and two others, with analogue functionality in one chip, CAFE, using a Bipolar process, and digital functionality in another, ABC, using a CMOS rad-hard process. Although still more work is required, both chip sets have come close to fulfilling the requirements, including radiation tolerance.

A fully-populated module of the barrel design, with ATLAS-specification Silicon microstrip sensors and the latest ABCD chip, ABCD2T, has been built and successfully shown to operate stably.

The SCT is in its final design phase and moving rapidly to the start of construction in 2001. A total of 19500 Silicon microstrip sensors are to be produced in 3 years, and assembled into 4500 modules in 2 years. The SCT is to be completed and installed by the beginning of 2004, and ATLAS is to be ready for experiment in the middle of 2005.

V. REFERENCES

- [1] The LHC Conceptual Design Report - The Yellow Book, CERN/AC/95-05(LHC) (1995)
- [2] ATLAS Technical Proposal for a General-Purpose pp Experiment at the Large Hadron Collider at CERN, CERN/LHCC/94-43 (1994)
- [3] E.g., ATLAS Inner Detector Technical Design Report Vol. 1, ATLAS TDR 4, CERN/LHCC 97-16 (1997); Vol. 2, ATLAS TDR 5, CERN/LHCC 97-17 (1997)
- [4] Fabricated by Hamamatsu Photonics Co. Ltd., Ichino, Hamamatsu 435-8558, Japan
- [5] H.-J. Ziock et al., Nucl. Instr. Meth. A342 (1994) 96-104
- [6] T. Ohsugi et al., Nucl. Instr. Meth. A342 (1994) 22-26
- [7] ABCD: Project specification ABCD2T/ABCD2NT ASIC version: V2.1, SCT collaboration, ATLAS
- [8] CAFE: Project specification CAFE-P Version: 4.01; ABC: Project specification ATLAS Binary Chip (ABC) Version: 5.01, SCT collaboration, ATLAS
- [9] Thermal Pyrolytic Graphite (TPG) made by Advanced Ceramics Corporation, P.O.Box 94924, Cleveland, Ohio 44101, U.S.A.
- [10] Geant4, a tool kit for the simulation of the passage of particles through matter, <http://wwwinfo.cern.ch/asd/geant4/geant4.html>